Electrical Power and Energy Systems 56 (2014) 316–324

Contents lists available at ScienceDirect

Electrical Power and Energy Systems

journal homepage: www.elsevier.com/locate/ijepes

Towards an extended power system stability: An optimized GCSC-based inter-area damping controller proposal

Amin Safari [a,*], Navid Rezaei [b]

[a] Department of Electrical Engineering, Ahar Branch, Islamic Azad University, Ahar, Iran
[b] Center of Excellence for Power System Operation and Automation, Electrical Engineering Department, Iran University of Science and Technology, Tehran, Iran

ARTICLE INFO

Article history:
Received 7 August 2012
Received in revised form 22 July 2013
Accepted 19 November 2013

Keywords:
Power system stability
Inter-area oscillation damping
Gate-Controlled Series Capacitor
Particle Swarm Optimization algorithm

ABSTRACT

Due to the crucial importance of the FACTS based damping controllers in mitigation the deteriorative impacts of the power system low frequency oscillations, particularly the inter-area modes, improving the system stability margins seems indispensible. This paper proposes an optimization approach to effectively carry out the multi-machine based stabilization function of the Gate-Controlled Series Capacitor (GCSC) in providing a robust damping to the power system low frequency oscillations. It is aimed to provide a reliable damping framework by means of an optimized GCSC based supplementary damping controller. Thus, to attain the most efficient set of the damping controller parameters, Particle Swarm Optimization algorithm as a proficient optimum hunter is employed to explore for the global stabilization solution in accordance to a vast range of power system operating conditions. Moreover, as a weighty assessment, the eigenvalue analysis is taken into account as the cornerstone of the performed studies in order to investigate the damping methodology in which the unstable or lightly damped inter-area modes are scheduled to effectively shift to some predominant stability zones in the s-plane. Meanwhile, derived results through the nonlinear time domain simulation as well as two dynamic performance evaluators manifestly demonstrate the impressiveness and verify the robustness of the proposed GCSC based damping scheme in enhancing the power system stability, especially regarding to the inter-area modes.

1. Introduction

Power system ever increasing demand for the secure and reliable electricity asks for intensified stability margins to be provided with an emergency priority in the system operation. On the other hand, regarding to the market restructuring and environmental constraints, power system stable performance especially fronting to the inherent low frequency oscillations (LFOs) is critical to the system operators. LFOs concerning to the mutuality of the system dynamic components lie in two major oscillatory modes. Inter-area modes with the frequencies in the range of 0.1–1 Hz and local modes having frequencies of 1–3 Hz ordain the power system low frequency oscillations [1,3]. Due to invaluable impacts of the steadily performance of the zonal tie lines in sustaining the system integrity and providing an incessant electrification, therefore, damping the inter-area modes appearing principally in large scale power systems has more preference to the local ones. The significance of damping the inter-area modes are when revealed that the conventional Power System Stabilizers (PSSs) are lacking in giving adequate relaxation to these modes, particularly in the case of heavy loading of the long transmission lines [1]. On the other hand, recently, Flexible AC Transmission System (FACTS) technology brings about a more universal stabilizing factor to the power systems. One of most utilities of the FACTS devices is the rapid controllability to provide a dynamic security limit in which at least the system inherent low frequency oscillations are mitigated guardedly. Hence, employing the FACTS controllers in such emphatic power systems is crucial to the system stability improvement [2,4]. Gate Controlled Series Capacitor (GCSC) treated as a new contribution of the FACTS series category is a potent power modulator producing dependable series compensation [5]. A single module of a GCSC comprises a capacitor connecting in shunt with a pair of anti-parallel gate-commutated switches. Wide range of controllability is the direct result of the gate-commutated based scheme. Furthermore, the GCSC by a structural-based restraining of the resonant frequencies unlike that occurs in the case of TCSC,[1] provides a continuous stabilizing signal standing to offer a more beneficial power system operation. For the sake of comparison to especially the TCSC and SSSC,[2] simplicity [6], extensive controllability [7] inexpensiveness [8] and high efficiency [9] are the main features led the

* Corresponding author. Address: Ahar City, Ahar and Tabriz Road km 2 - Ahar Branch, Islamic Azad University, Zip: 5451116714. Tel./fax: +98 4262235438.
E-mail addresses: a-safari@iau-ahar.ac.ir (A. Safari), nrezaei@iust.ac.ir (N. Rezaei).

[1] Thyristor Controlled Series Capacitor.
[2] Static Synchronous Series Compensator.

0142-0615/$ - see front matter © 2013 Elsevier Ltd. All rights reserved.
http://dx.doi.org/10.1016/j.ijepes.2013.11.028

GCSC to be considered as a powerful option in enhancing the system dynamic stability. Although considering to the further practical background of the TCSC and its more familiar operative aspects, referring to the overall controllability of the gate commutated switches, the GCSC, at least from the theoretical viewpoint, has more profitableness to its elder scheme, i.e. TCSC. It should be noted that all the aforementioned comparisons are valid only using the mathematical hypotheses, and in the operational phases, at this time, the GCSC may be a risky choice, however it seems erelong to have an appropriate potential to be adopt in the real experiences. Consequently, it could be said that the GCSC may be soon replaced by the TCSC or even SSSC in most of series compensation scopes. As reported in the literature, to improve a better damping to the power system, some commonly modern control methodologies such as fuzzy set [10] and neural networks [9] are developed to design a GCSC based damping controller. Although these algorithms are impressive, but they are on the basis of the trial and error efforts especially in the initialization stages and in some cases, may cause to reach improper solutions. Although, the investigation the power system dynamic performance has been performed in some literatures [6,9,10], the lacuna of a detailed and thorough study on the GCSC, as an appropriate series compensator, efficient dynamic modeling and damping performance analysis, especially regarding to the low frequency oscillations is still evident. In order to fill this gap out, the main contribution of the paper is in the light of proposing a detailed proper dynamic modeling of the GCSC to investigate perfectly the capability of the GCSC in providing a robust damping framework to the power system LFOs.

To augment the modulated damping torque of the GCSC against the system uncertainties and nonlinear interactions and also attain a more techno-economical operation of the GCSC modules, a supplementary damping controller is proposed to be designed in a way in which the GCSC stabilizing signal is reinforced. In this study, an industrial preferable scheme of the damping controllers is proposed to be determined optimally. The present paper uses Particle Swarm Optimization (PSO) algorithm to search for the optimistic set of damping controller parameters. The PSO is known as a straightforward search conductor seeks intelligently for the near global optimal destination. Because of impassible nature of the PSO to the particularly nonlinear, differential and large scale problems [11], and further referring to the multi-modal fulfillment of the controller parameters, it is seemed to be an appropriate candidate to solve the problem of damping controller design. The problem of eliciting the optimistic set of controller parameters using the PSO algorithm is transmitted into a minimization an eigenvalue based fitness function. The purpose is to robustly shift the un-damped or lightly damped eigenvalues to some specified stable regions in the s-plane. It should be noted that due to more importance of the inter-area modes, only the dominant corresponded inter-area eigenvalues with frequencies in the range of 0.1–1 Hz are derived and be analyzed via the fitness function ruler. Hence, a multi-machine two area power system is considered to be equipped with the GCSC and then the stability issue is evaluated over the test system using the nonlinear dynamic equations. Owing to the capability of the current injection model in rendering a more detailed dynamic model of the FACTS devices, it is selected to be used in dynamic modeling of the GCSC. High compatibility, universality and easy implementation in the system dominant studies like OPF and stability analyses motivate to employ the current injected based model for GCSC in this contribution [21]. Besides, to guaranty the robustness and competency of the optimized damping controller, a wide range of operating points is assumed to be applied to the test power system. Moreover, to assure the controller performance a severe transient disturbance is imposed to the power system and the corresponding results are demonstrated in the framework of nonlinear time domain simulations.

The paper approach focuses on estimation the GCSC capability in providing a more robust stabilizer function for a multi-machine power system. Thus, a supplementary damping controller is assumed to be optimally designed in order to strengthen the GCSC modulating damping torque. The PSO algorithm is assigned to find the optimistic set of damping controller parameters through minimizing some eigenvalue based fitness functions over a wide range of operating conditions. Also, the nonlinear time domain simulation is employed to validate the eigenvalue analysis results. Assessment the derived results clearly show the efficiency of the GCSC in enhancement the system stability. Moreover, by calculation the numerical values of two performance indices defined on the basis of the power system dynamic response to the assumed disturbance, it can be deduced that all of the considered fitness functions provide a suitable stabilizing signal not only for the inter-area modes but also the local modes are damped aptly. To assure of the optimization results derived from the PSO, the performance of the PSO algorithm in the terms of the convergence rate and also the computational time is compared to the GA algorithm. The superiority of the PSO-based results validates the optimized tuning of the damping controller parameters and verifies the secure system stability improvements.

2. Description the system under study

2.1. Gate Controlled Series Capacitor

According to the substantial effects of the GCSC in increasing the power system available transfer capability (ATC) and thereby, providing more developed system stability margins, it is necessary to exploit a detailed and as well a compatible model to the nonlinear ingredients of a practical large scale power system. In this quest, the current injection model of the GCSC is drawn out through the variable impedance model. Truism, as represented in Fig. 1 for the GCSC installed between the buses i and j, the equivalent impedance is a variable capacitance changeable by the switch blocking angle variations. It is notable that the activate series compensation is produced when the blocking angle varies in range of 0–90° with respect to the line current maximum point [12].

Eq. (1) explains the relationship between the GCSC capacitive reactance and the blocking angle γ [2,12]. In Fig. 2 the equivalent impedance model of the GCSC is shown.

$$X_{GCSC}(\gamma) = X_C\left(1 - \frac{2\gamma}{\pi} - \frac{\sin(2\gamma)}{\pi}\right) \tag{1}$$

To attain the proposed current injection model, first the series current which flows through the compensated transmission line is considered to be calculated according to Fig. 2 as following:

$$\bar{I}_{se} = \frac{\overline{V}_i - \overline{V}_j}{r_l + j(x_l - x_{GCSC}(\gamma))} \tag{2}$$

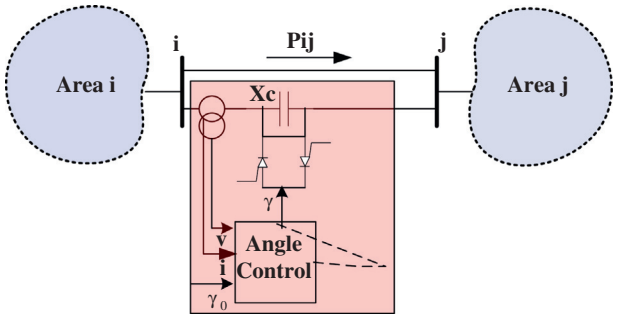

Fig. 1. The GCSC installed between buses i and j.

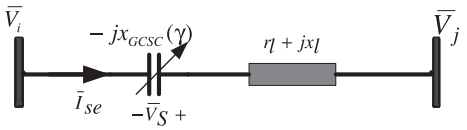

Fig. 2. The equivalent circuit of the GCSC installed between buses *i* and *j*.

where the voltage phasors of the buses *i* and *j*, the resistance and reactance of the transmission line and the variable GCSC reactance are represented by $\overline{V}_i, \overline{V}_j, r_l, x_l$ and $x_{GCSC}(\gamma)$, respectively. The next stage is to replace the series variable voltage source ($\overline{V}_S$) by an equivalent shunt current source as shown in Fig. 3a. Finally, by calculating the injected current of the buses i and j, the current injection model is extracted. Fig. 3b represents the final version of the GCSC current injection model. The calculations are as follows:

$$\overline{V}_s = -jx_{GCSC}\overline{I}_{se} \tag{3}$$

$$\overline{I}_s = \frac{\overline{V}_s}{r_l + jx_l} = \frac{-jx_{GCSC}\overline{I}_{se}}{r_l + jx_l} \tag{4}$$

$$\overline{I}_{si} = \frac{-jx_{GCSC}}{r_l + jx_l} \cdot \frac{\overline{V}_i - \overline{V}_j}{r_l + j(x_l - x_{GCSC})} \tag{5}$$

$$\overline{I}_{si} = -\overline{I}_{sj} \tag{6}$$

Notably, the derived current injected based model preserves the system nominal admittance matrix and consequently facilitates the process of nonlinear dynamic simulations [4,13]. Furthermore, substitution in the system current matrix and conservation the system admittance matrix, cause the faster computational time and more precise dynamic performance improvement [21].

2.2. Multi-machine test power system

To investigate the damping performance of the GCSC, particularly regarding to the mitigation the inter-area oscillations, a four machine two area test power system as shown in Fig. 4 is assumed to be simulated. The system relevant data is given in [3]. The simulated nonlinear dynamics of the *i*th machine are [3,14]:

$$\dot{\delta}_i = \omega_0(\omega_i - 1) \tag{7}$$

$$\dot{\omega}_i = \frac{P_{mi} - P_{ei} - D_i(\omega_i - 1)}{M_i} \tag{8}$$

$$\dot{E}'_{qi} = \frac{E_{fdi} - (x_{di} - x'_{di})i_{di} - E'_{qi}}{T'_{doi}} \tag{9}$$

$$\dot{E}_{fdi} = \frac{K_{Ai}(V_{refi} - V_{ti}) - E_{fdi}}{T_{Ai}} \tag{10}$$

$$T_{ei} = E'_{qi}i_{qi} - (x_{di} - x'_{di})i_{di}i_{qi} \tag{11}$$

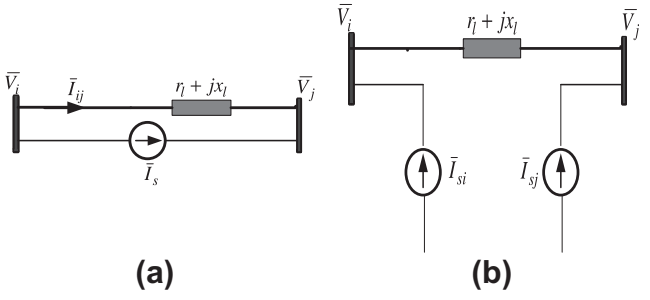

Fig. 3. The GCSC current injection model. (a) Substitution the shunt current source. (b) Extraction the current injection sources.

where δ, ω, P_m, P_e, E'_q, E_{fd}, T_e, T'_{do}, K_A, T_A, V_{ref} and V_t denote rotor angle, rotor speed, mechanical input power, electrical output power, internal voltage behind x'_d, equivalent excitation voltage, electric torque, time constant of excitation circuit, AVR gain, AVR time constant, reference voltage and terminal voltage, respectively. It is worth mentioning that the power system is operated with all the essential and itemized stability required dynamics. Dynamic aspects of the system are thoroughly investigated with respect to the localized measuring signals, and thus in light of the detailed dynamics assessment, though, it is not as comprehensive as a large scale realistic power system, the basic characteristics and detailed interactive performance of the system controllers can be well estimated and the extracted conclusions through an insight perspective may be eligible to effectively generalize for implementation in the high dimensional test power systems [20,21].

3. The proposed approach

3.1. The structure of the supplementary damping controller

For the sake of upgrading the efficiency of the GCSC in producing an intensified damping torque, has need to employ an assistant damping controller with the aim of achieving an economical operation of the GCSC. It is notable that as for the simplicity, availability and adaptability of the classic lead – lag controllers, they are still preferred by the electrical utilities [15]. A signal washout block, a gain block and two-stage phase compensator block are the foundational construction of the commonly used lead – lag supplementary controller. The controller design main scope is to provide a robust phase lead compensator to make up for the phase lag between input and output signals [16]. This implies optimal determination of K, T_1, T_2, T_3 and T_4 parameters. The block-diagram of the utilized GCSC-based damping controller is depicted in Fig. 5. T_W is the washout time constant which typically takes a value in the range of 1–20 s [15,16] and here is set within 10 s. T_{GCSC} denotes the natural time delay of the blocking angle inside controller impacted in the GCSC module and is selected within 20 ms. X_0, X_{min} and X_{max} represent the GCSC reactance at initial set-point corresponding to the angle γ_0, lower limit of the GCSC reactance matched to the angle $\gamma = 90°$ and upper limit of the GCSC reactance rises from the angle $\gamma = 0°$, respectively.

The tie-line active power (P12) transferred between the two areas is selected here to be used as the proposed controller input signal. That is why this local signal contains invaluable information about the inter-area modes and is more adaptable to the application of the FACTS series controllers [13].

3.2. Optimization formulation

As mentioned earlier the problem of the proposed damping controller design is a multi-modal which means that has more than one local optimum solution. Therefore, it is proper to employ an adequate optimization algorithm to find the global optimal solution of the design problem. In this study, Particle Swarm Optimization algorithm has undertaken solving the optimization. Thus, the problem of determining the set of damping controller parameters is transmitted to minimization of some eigenvalue based fitness functions in which the purpose is to suitably shift the unstable or lightly damped inter-area eigenvalue to some robust stable areas in the s-plane. Worth to mention that the eigenvalue analysis is currently an efficient indicator to the power system stability issues. The fitness functions are specified as the following F_1, F_2 and F_3 functions:

$$F_1 = \sum_{i=1}^{NP} \sum_{\sigma_k \geq \sigma_0} (\sigma_{k,i} - \sigma_0)^2; \quad \sigma_{k,i} = \mathrm{Re}\ al(\lambda_{k,i}) \tag{12}$$

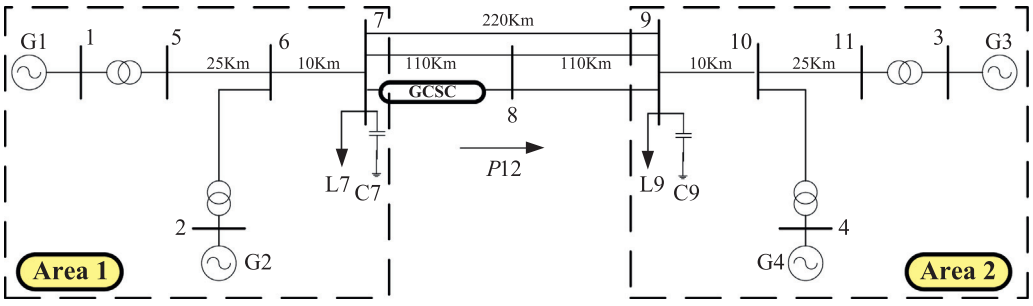

Fig. 4. The two area four machine test power system equipped with the GCSC.

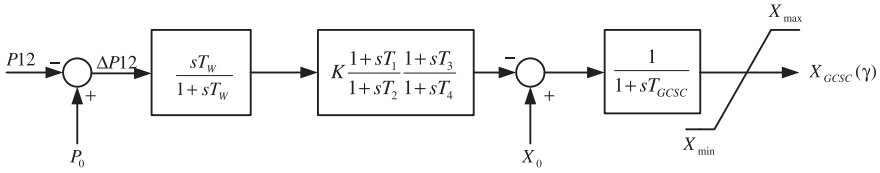

Fig. 5. The structure of the proposed damping controller.

$$F_2 = \sum_{i=1}^{NP} \sum_{\xi_k \le \xi_0} (\xi_{k,i} - \xi_0)^2; \quad \xi_{k,i} = -\text{Re } al(\lambda_{k,i})/|\lambda_{k,i}| \tag{13}$$

$$F_3 = \sum_{i=1}^{NP} \left[\sum_{\sigma_k \ge \sigma_0} (\sigma_{k,i} - \sigma_0)^2 + \rho \cdot \sum_{\xi_k \le \xi_0} (\xi_{k,i} - \xi_0)^2 \right]; \quad \rho = 10 \tag{14}$$

where $\lambda_{k,i}$, $\sigma_{k,i}$, $\xi_{k,i}$ are stands for kth eigenvalue, real part of the kth eigenvalue and the damping ratio of the kth eigenvalue, all in the ith operating point, respectively. σ_0 and ξ_0 are pre-specified real part and damping ratio which are assumed to lead the system unstable and lightly damped inter-area eigenvalues to the considered stability areas depicted in Fig. 6. The values of σ_0 and ξ_0 are -2 and 0.45 in this study. *NP* represents the total number of operating points assumed to carrying out the system performance regarding to them. Meanwhile, it is scheduled to match the F_1, F_2 and F_3 functions to the areas demonstrated in Fig. 6a–c, respectively. Moreover, to be sure of global achieving the optimistic solution it is necessary that the PSO is performed under a wide range of operating conditions. Table 1 gives the assumed operating points obtained using the multi-machine load flow analysis. The operating points have been tried to be picked in a way that the marginal load-ability and generation levels could be simulated through the load flow analysis.

It is considered that the aforementioned fitness functions be optimized subject to the following bounded constraints:

$$\begin{aligned} &0 < K < 200 \\ &0.01 < T_x < 2, \quad x = 1,2,3,4. \end{aligned} \tag{15}$$

4. Review of the Particle Swarm Optimization algorithm

The main execute phases of the PSO algorithm can be explained through the following [17–19]:

4.1. Phase 1: Initialization

Step 1: Choose the values of the PSO basic parameters (swarm population size, particle dimensions, cognitive and social coefficients, condition(s) for ending the search process).
Step 2: Generate randomly the initial swarm position and velocity matrices with i particles in a D-dimensional search space.

4.2. Phase 2: Fitness function evaluation

Step 3: Apply the specified fitness function(s) to evaluate the suitability of each particle.
Step 4: Determine the best local value(s) (*pbest*) and global value (*gbest*) via the fitness function(s) scale.

4.3. Phase 3: Updating the optimization agenda

Step 5: Update the swarm position and velocity.
Step 6: Evaluate again the particles through the fitness function(s) criteria and replace the *pbest* and maybe the *gbest*; (if the new *gbest* has better propriety index, the former *gbest* is still preserved up to the next appraisal is administered).

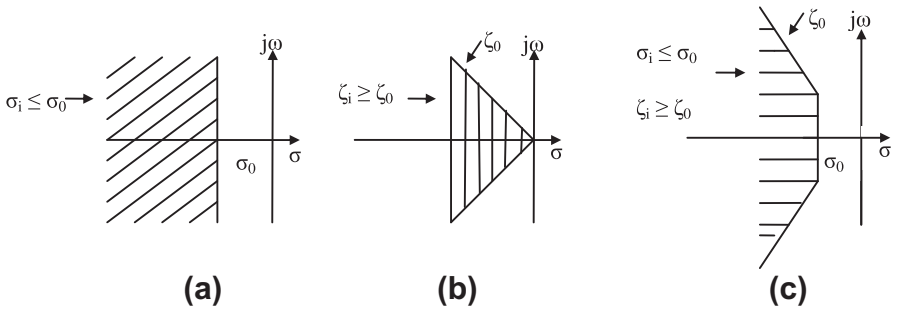

Fig. 6. Regions of eigenvalue locations for different objective functions.

Table 1
The considered power system operating points.

Operating point	P_1	Q_1	P_2	Q_2	P_3	Q_3	P_4	Q_4
Case 1	0.7621	0.0835	0.7176	0.0671	0.8226	0.1331	0.7927	0.1362
Case 2	0.9061	0.1639	0.7667	0.1934	0.7333	0.0732	0.7000	0.0764
Case 3	0.5050	0.0519	0.9067	0.1155	0.8889	0.1163	0.8778	0.1065

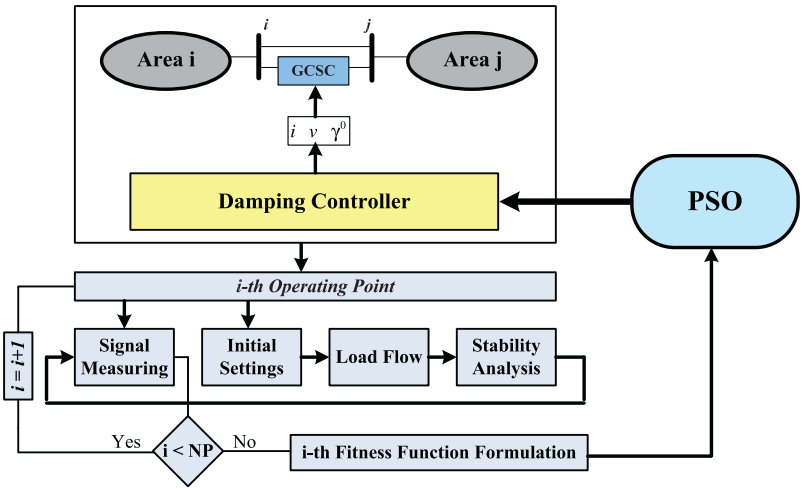

Fig. 7. The process of optimal tuning of the damping controller parameters using the PSO algorithm.

Table 2
Optimized set of damping controller parameters for different fitness functions.

	K	T_1	T_2	T_3	T_4
F_1	87.12	0.0751	0.6610	0.9855	0.9003
F_2	40.01	1.2556	0.0182	0.2116	1.0280
F_3	194.63	0.0859	0.0442	1.6237	1.9025

4.4. Phase 4: Checking the harvest home condition(s)

Step 7: Check the condition(s) for ending the search procedure; if it has been satisfied, harvest the global optimum solution, else go to the step 3.

The performance of the particles in the PSO algorithm can be described using Eqs. (16)–(18) [18].

$$v_{id}(t+1) = \omega v_{id}(t) + c_1 rand_1(pbset(t) - x_{id}(t)) + c_2 rand_2(gbest(t) - x_{id}(t)) \quad (16)$$

$$\vec{x}(t+1) = \vec{x}(t) + \vec{v}(t+1) \quad (17)$$

where x_{id}, v_{id}, *pbset* and *gbest* are identifies the position, velocity, local optimum of each particle and global optimum of the group, respectively [18]. c_1 and c_2 are cognitive and social acceleration coefficients, respectively by which the adaptability with the global best particle is clearly indicated. To control the convergence ratio, especially in the last iterations, an inertia weight is set as ω in Eq. (18) [11,18]. The value of ω is decreased linearly from 0.9 to 0.4 during the assumed iterations (*iter*).

$$\omega = \omega_{max} - \frac{\omega_{max} - \omega_{min}}{iter_{max}} \cdot iter \quad (18)$$

In this study, number of swarm particles, number of iterations, cognitive and social coefficients are chosen as 50, 100, 2 and 2, respectively. To verify that the PSO parameter sets (i.e. c_1 and c_2) are designated in a reliable way which fits to the study, different set of the c_1 and c_2 parameters are picked and the best value of the fitness functions are computed. Moreover, the optimization process using PSO is illustrated in Fig. 7. The damping controller parameters (K, T_1, T_2, T_3 and T_4) are tuned using the PSO algorithm and considering to data exchanged with the simulated power system in the SIMULINK environment. In other words, a 5-dimension particle (i.e. damping controller parameters) is generated by the PSO paradigm, iteratively. Then the proposed parameters are applied to the simulated 2-area test power system in the SIMULINK model and for every operating point corresponding to Table 1, the load flow and stability analyses are ran and the dominant signals of the power system (ω_i and P12) are measured to formulate the fitness function (F_i). Then if the proposed damping controller parameters are optimized the fitness function and satisfied the boundary constraints in Eq. (15), they are selected as the optimal solutions and preserved to be compared to the other generation

Table 3
The shifted inter-area eigenvalues with corresponding frequency and damping ratios.

Fitness functions	*Without controller*	F_1	F_2	F_3
Case 1	0.11 ± 4.59*i*, 0.73, −0.02	−2.01 ± 4.60*i*, 0.74, 0.4 −5.18 ± 1.29*i*, 0.21, 0.97	−1.41 ± 2.71*i*, 0.48, 0.47 −27.27 ± 2.49*i*, 0.44, 0.99	−2.55 ± 1.62*i*, 0.23, 0.84 −11.67 ± 2.41*i*, 0.34, 0.97
Case 2	0.12 ± 6.12*i*, 0.973, −0.02 −22.51 ± 2.73*i*, 0.43, 0.99	−2.01 ± 4.98*i*, 0.85, 0.37 −5.45 ± 0.64*i*, 0.1, 0.99 −22.53 ± 1.01*i*, 0.16, 0.99	−1.70 ± 3.34*i*, 0.53, 0.46 −22.66 ± 0.99*i*, 0.16, 0.99	−3.21 ± 2.66*i*, 0.42, 0.76 −12.16 ± 1.99*i*, 0.31, 0.98 −22.67 ± 0.95*i*, 0.15, 0.99
Case 3	0.12 ± 4.64*i*, 0.74, −0.03 −23.01 ± 2.73*i*, 0.43, 0.99	−2.04 ± 4.95*i*, 0.76, 0.36 −5.24 ± 0.99*i*, 0.15, 0.98	−1.82 ± 2.88*i*, 0.54, 0.53 −27.64 ± 2.57*i*, 0.48, 0.99	−2.67 ± 1.48*i*, 0.23, 0.87 −12.01 ± 1.93*i*, 0.31, 0.98

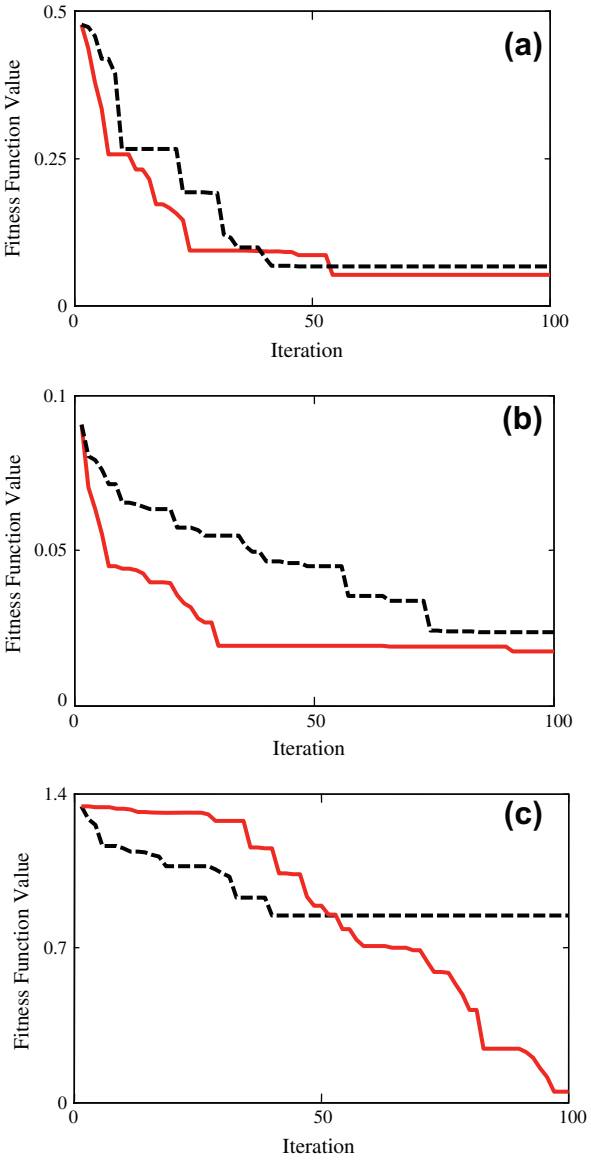

Fig. 8. The convergence ratio for F_1 (a), F_2 (b) and F_3 (c). Fitness function with GA (dashed) and PSO (solid) Algorithms.

of the parameters. If a better solution in the viewpoint of the fitness function criterion is obtained the optimal solution will be updated. At the end of the pre-scheduled iterations, the optimal set of the parameters which are the same as the *gbest* value in the PSO paradigm are found out and prepared to be used in the damping controller structure in Fig. 5. to stabilize the power system against the severe disturbances.

5. Simulation results

In this study, the process of the GCSC based damping controller design is formulated to an optimization problem which is proposed

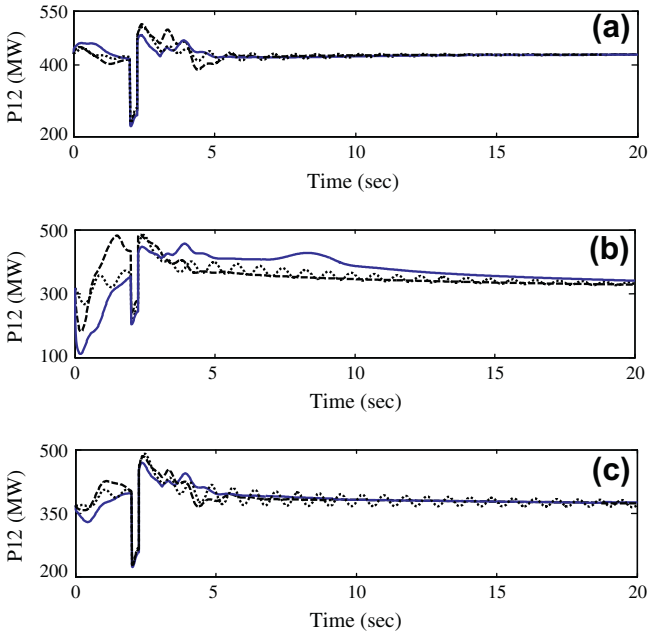

Fig. 9. Dynamic response of tie-line power transfer signal (P12) in (a) Case 1, (b) Case 2 and (c) Case 3: solid (F_3), dashed (F_2) and dotted (F_1).

to be solved by the PSO algorithm. Indeed, each particle in the PSO search space plays as a set of the proposed damping controller parameters. In order to determine the optimistic corresponding values of each particle and on the basis of the eigenvalue analysis, it is considered to calculate the value of each F_1, F_2 and F_3 fitness functions for each particle under various assumed operating conditions. The global-optimum set of the parameters are picked after several iterative evaluations among local optimums. Then, it is expected for this set of the selected parameters the proposed controllers will have the best damping performance and robustly stabilizes the system oscillations. Furthermore, the nonlinear time domain simulation is performed to validate the eigenvalue analysis results.

The parameters of damping controller, i.e. K, T_1, T_2, T_3 and T_4 which are optimized via the PSO algorithm in order to provide an efficient power system stability operation are listed in Table 2. which indicates the optimized set of the damping controller parameters which are carried out for the F_1, F_2 and F_3 functions and concerning to the given operating points in Table 1. Also, the shifted inter-area eigenvalues corresponding to the F_1, F_2 and F_3 functions with their frequency and damping ratios are shown in Table 3. The criterions of the specified stability regions as illustrated in Fig. 6 have all been satisfied in the optimization procedure.

Furthermore, in order to validate the PSO-based optimization process, the performance of the PSO algorithm corresponding to each fitness function is compared to the GA algorithm. The convergence ratios are depicted in Fig. 8, and the computational results are given in Table 4. Results are clearly reveal the superior performance of the PSO algorithm and verifies the optimization process of selection the set of the damping controller parameters.

Table 4
The optimization results of the PSO and GA algorithms considering to the different fitness functions evaluation.

Evaluation index	Best value			Mean value			CPU time (s per iteration)		
Fitness function	F_1	F_2	F_3	F_1	F_2	F_3	F_1	F_2	F_3
GA	0.130	0.032	0.882	0.366	0.044	0.979	380	333	608
PSO	0.118	0.021	0.187	0.249	0.026	0.501	321	296	466

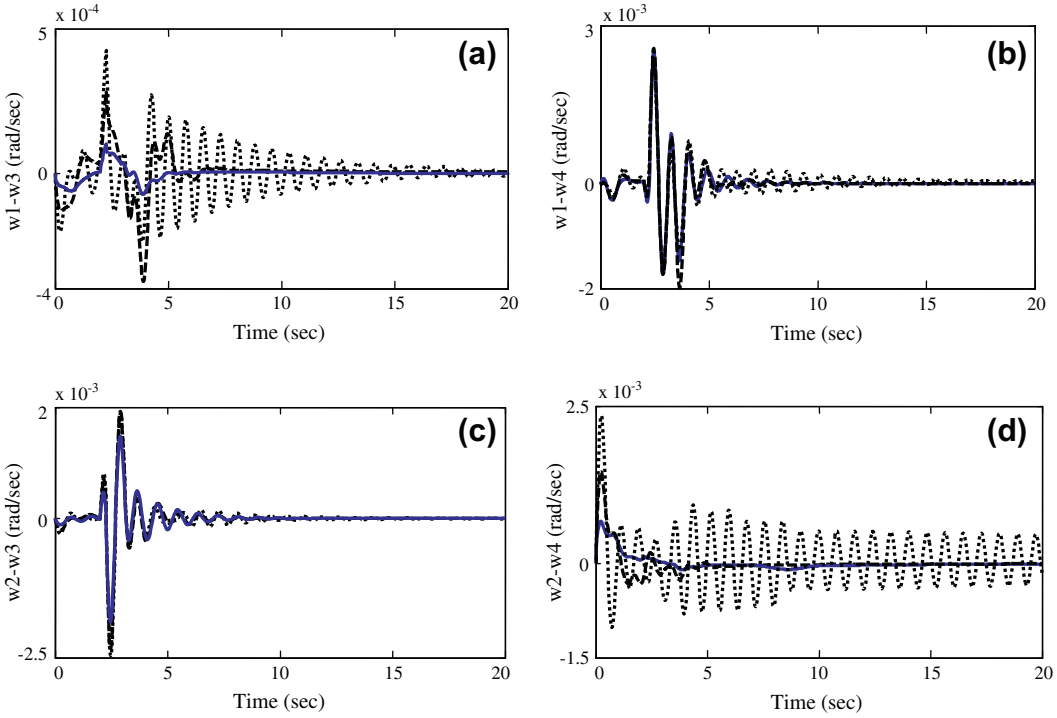

Fig. 10. The power system inter-area rotor speed responses to the disturbance in Case 1: solid (F_3), dashed (F_2) and dotted (F_1).

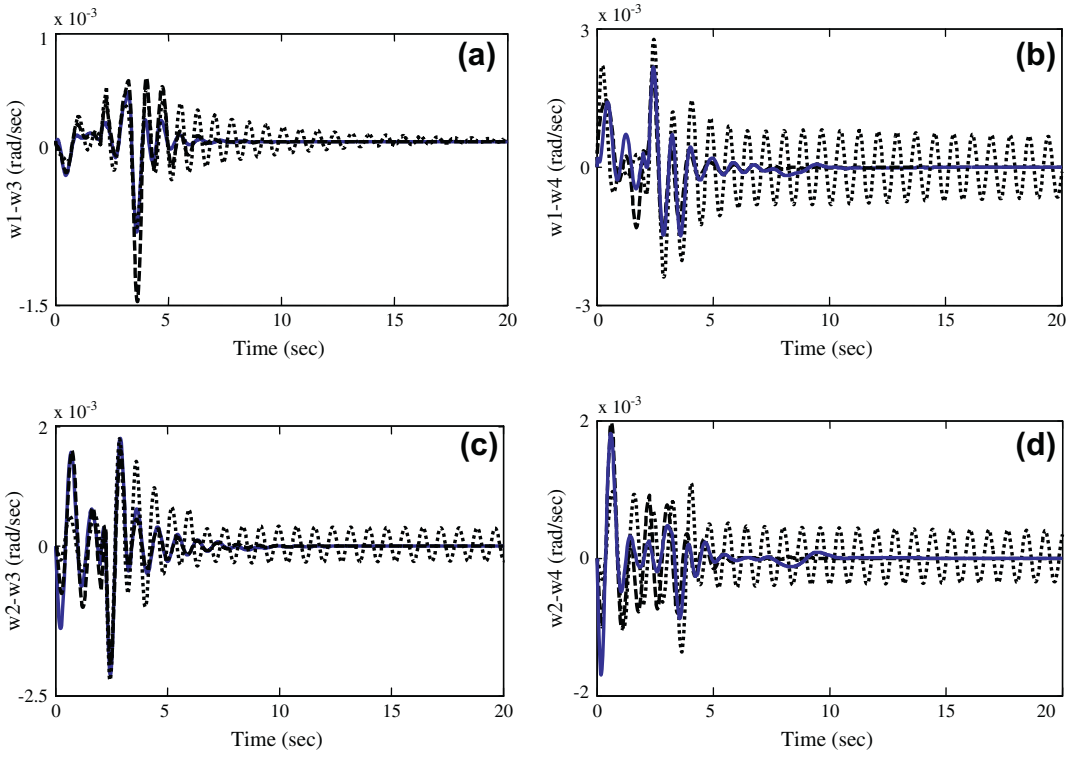

Fig. 11. The power system inter-area rotor speed responses to the disturbance in Case 2: solid (F_3), dashed (F_2) and dotted (F_1).

Moreover, to better assess the robustness of the designed damping controllers, it is assumed that a severe disturbance is imposed to the test power system. In this disturbance, it is tried to investigate the system performance under more difficult disturbance. Thus, a severe three-phase fault is assumed to be occurred at $t = 2$ s and in the middle of the transmission line between the buses 7 and 9. It is considered the fault is cleared after 250 ms and by permanently tripping of the faulted line. To validate the simulated results of the eigenvalue analysis, the nonlinear time domain simulation is taken into account. Fig. 9 represents the tie-line power transfer variations (P12) in response to the assumed disturbance and in the considered operating conditions. Furthermore,

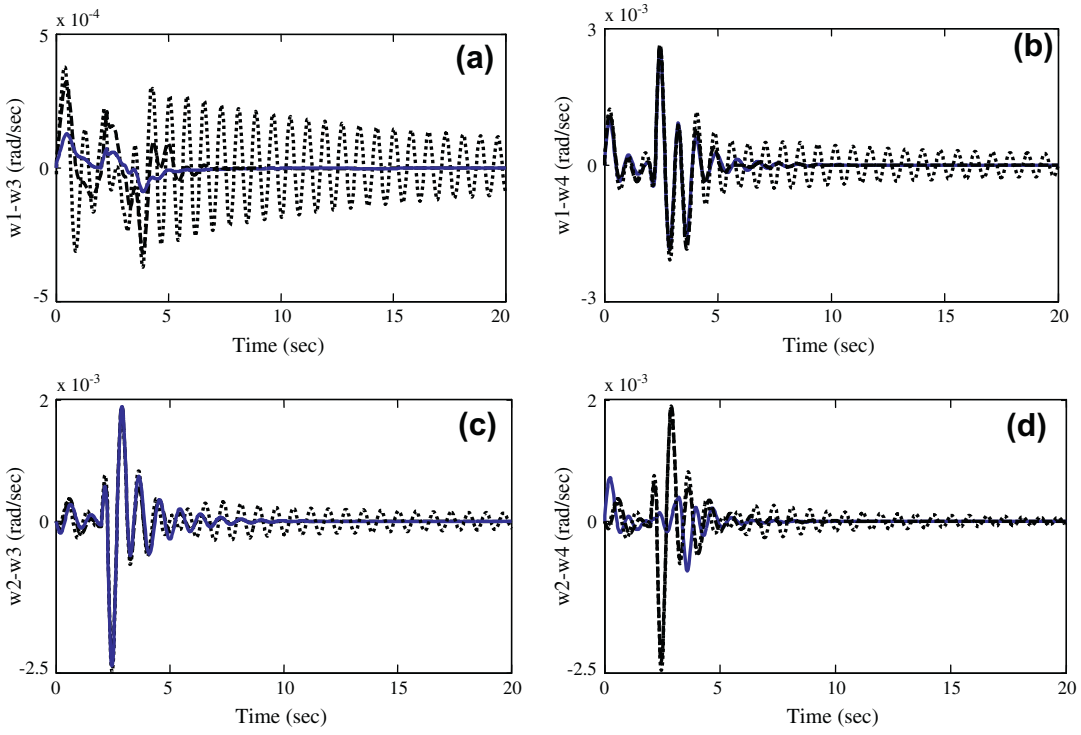

Fig. 12. The power system inter-area rotor speed responses to the disturbance in Case 3: solid (F_3), dashed (F_2) and dotted (F_1).

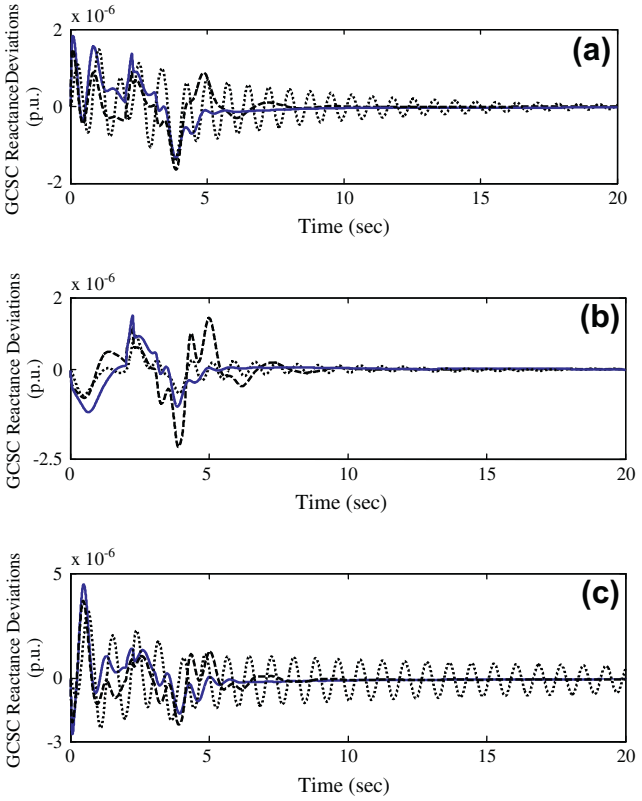

Fig. 13. The GCSC reactance deviations in (a) Case 1, (b) Case 2 and (c) Case 3: solid (F_3), dashed (F_2) and dotted (F_1).

the relative inter-area machine speed deviations are depicted in Figs. 10–12 regarding to the disturbance effect in all operating conditions. To better demonstrate the damping controller performance the GCSC reactance deviations according to fitness functions are also depicted in Fig. 13.

In order to better verify the derived results through the eigenvalue analysis and the time domain based simulation, two efficacious performance indices (*P.I.*) as defined in Eqs. (19) and (20) are employed. The performance indices are on the basis of dynamic response of the power system to the considered disturbance during the simulation framework. The *I.P.I* is taken into account to estimate the damping measure of the inter-area modes and similarly the *L.P.I* evaluates the local modes damping index. Worth mentioning that the lower values of the each *P.I.* indicate the better stability functions.

$$I.P.I. = 100\int_0^{tsim} t\cdot\left(\sum \Delta\omega_I\right)dt = 100\int_0^{20} t\cdot(|\omega_1-\omega_3| + |\omega_2-\omega_3| + |\omega_2-\omega_4| + |\omega_1-\omega_4|)dt \quad (19)$$

$$L.P.I. = 100\int_0^{tsim} t\cdot\left(\sum \Delta\omega_L\right)dt = 100\int_0^{20} t\cdot(|\omega_1-\omega_2| + |\omega_3-\omega_4|)dt \quad (20)$$

where *tsim* and ω_i depict the performed simulation time and the *i*th machine rotor speed signal, respectively. Meanwhile, $\Delta\omega_I$ and $\Delta\omega_L$ are representative the rotor speed deviations for the inter-are oscillatory modes and the local ones, respectively. In Fig. 14, the numerical results of the aforementioned performance indices are demonstrated in all operating conditions and corresponding to each fitness function.

Obviously, as same it is represented in the time domain simulations, the F_3 fitness function which has regarded the stabilizing characteristics of the both F_2 and F_1 fitness functions gets more efficient power system damping comparing to the F_2 and F_1 functions. In short, the F_3 plays as a beneficial multi-objective fitness function applied to the test power system and consequently anticipated to provide more extent stability margins. From the performance index based numerical results can be inferred that the all

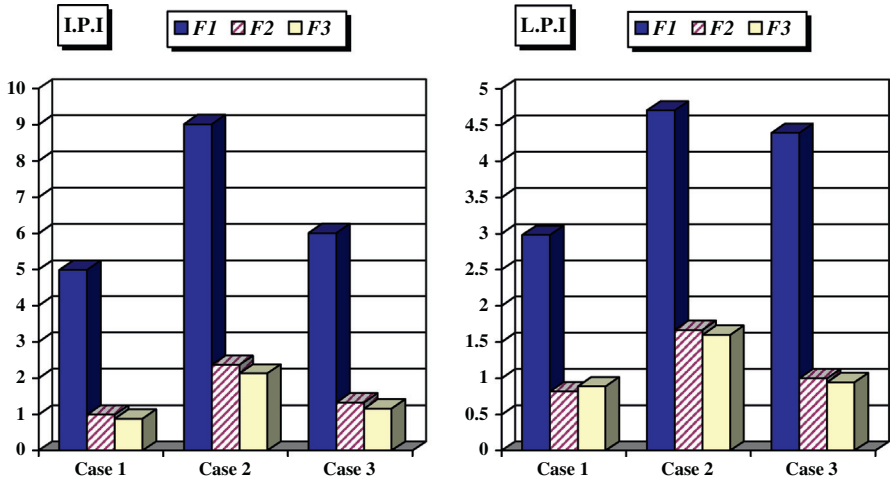

Fig. 14. The *I.P.I* and *L.P.I* numerical results.

designed damping controllers not only damp imperatively the inter-area modes but they also are advantageous in providing adequate damping for the local modes. Furthermore, the capability of the proposed current injection model is revealed throughout the derived simulations. In a noteworthy manner, the optimized GCSC based damping framework is invaluable in providing more strengthened power system stability criterion especially to the inter-area modes and by equipping the power system with the GCSC and injecting the damping modulation currents to the system, the electromechanical swings have been well controlled and the stability margins of the power system have been enhanced to the tailored levels.

6. Conclusions

The present paper contributes to investigate the GCSC damping function in enhancing the stability margins of a multi-machine power system. In order to better dynamic operation of the GCSC, the current injection model was utilized. Then, an optimization problem was formulated considering to a wide range of operating conditions and the PSO algorithm employed to solve the problem optimistically. The PSO was aimed to minimize some eigenvalue based fitness functions in which the unstable and/or lightly damped inter-area oscillations shifted to some per-scheduled stable zones in the s-plane. The optimal set of the damping controller parameters were applied to the test power system and the simulation results were drawn out. The simulation results regarding to a severe disturbance and in terms of eigenvalue analysis, nonlinear time domain simulation and numerical performance indices are all evidently verify the robustness and effectiveness of the designed GCSC based damping controller in adequately mitigation of the inter-area oscillatory modes. Furthermore, the results demonstrate the imperative effect of the current injection model of the GCSC in enhancing the power system stability.

References

[1] Padiyar KR. FACTS controllers in power transmission and distribution. India: New Age Publishers; 2007.
[2] Hingorany N, Gyugyi L. Understanding FACTS: concepts and technology of flexible AC transmission systems. IEEE Press 2000.
[3] Kundur P. Power system stability and control. New York: McGrew Hill; 1994.
[4] Sadikovic R. Use of FACTS devices for power flow control and damping of oscillations in power systems. Ph.D. thesis, Swiss Federal Institute of Technology; 2006.
[5] Karady GG, Ortmeyer TH, Pilvelait BR, Maratukulam D. Continuously regulated series capacitor. IEEE Trans Power Deliv 1993;8(3):1348–55.
[6] De Souza LFW, Wanatabe E, De Jesus D. SSR and power oscillation damping using gate-controlled series capacitors. IEEE Trans Power Deliv 2007;22(3):1806–12.
[7] De Souza LFW, Wantanabe E, Alves JER. Thyristor and gate-controlled series capacitor: a comparison of components ratings. IEEE Trans Power Deliv 2008;23(2):899–906.
[8] Ardes M, Portela C, Emmerik ELV, Da Silva Dias RF. Static series compensators applied to very long distance transmission lines. Electr Eng 2004;86(2):69–76.
[9] Ray S, Venayagamoorthy GK, Watanabe EH. A computational approach to optimal damping controller design for a GCSC. IEEE Trans Power Deliv 2008;23(3):1673–81.
[10] Alizadeh Pahlavani MR, Mohammadpour HA. Damping of sub-synchronous resonance and low frequency power oscillations in a series-compensated transmission line using gate-commutated series capacitor. Electr Power Syst Res 2011;81(2):308–17.
[11] Del Valle Y, Venayagamoorthy GK, Mohagheghi S, Carlos J, Harlry RG. Particle swarm optimization: basic concepts, variants and application in power systems. IEEE Trans Evol Comput 2008;12(2):171–95.
[12] Wanatabe EH, Aredes M, Barbosa PG, Santos G, De Lima FK, Da Silva Dias RF. Flexible AC transmission system. Power electronics handbook. Elsevier; 2007. p. 797–822.
[13] Shayeghi H, Shayanfar HA, Jalilizadeh S, Safari A. TCSC robust damping controller design based on particle swarm optimization for a multi-machine power system. Energy Convers Manage 2010;51(10):1873–82.
[14] Yu YN. Power system dynamics. Academic Press; 1983.
[15] Talaq J. Optimal power system stabilizers for multi machine systems. Int J Electr Power Energy Syst 2012;43(1):793–803.
[16] Ali ES, Abd-Elazim SM. Coordinated design of PSSs and TCSC via bacterial swarm optimization algorithm in a multimachine power system. Int J Electr Power Energy Syst 2012;36(1):84–92.
[17] Eberhart R, Kennedy J. A new optimizer using particle swarm theory. Micro Mach Hum Sci 1995:39–43.
[18] Shi XY. Introduction to mathematical optimization from linear programming to meta-heuristics. Cambridge International Science Publishing; 2008.
[19] Ratnaweera A, Halgamuge SK, Watson HS. Self organizing hierarchical particle swarm optimization with time varying acceleration coefficients. IEEE Trans Evol Comput 2004;8(3):240–55.
[20] Panda S. Robust coordinated design of multiple and multi-type damping controller using differential evolution algorithm. Int J Electr Power Energy Syst 2011;33:1018–30.
[21] Rezaei N, Kalantar M, Shayanfar HA, Alipouri Y, Safari A. Optimal signal selection and damping controller design for IPFC using a novel current injection model in a multi-machine power system. Int J Electr Power Energy Syst 2013;44(1):461–70.